International Journal of Control, Energy and Electrical Engineering (CEEE)
Vol.7 pp.18-23

Control in Stand-alone Wind Energy Conversion System Using Vector Control of DSIG

Samira Aitouaret Chekkal, Narimen Aouzellag Lahaçani, Djamal Aouzellag, Kaci Ghedamsi

Département Génie Electrique, Université de Bejaia
Bejaia 06000, Algeria
samirachekkal@yahoo.fr
nlahacani@yahoo.fr
aouzellag@hotmail.com
kghedamsi@yahoo.fr

***Abstract*— This paper presents the operation of a stand-alone wind energy conversion system using a Dual-Stator Induction Generator (DSIG) as well as the contribution they can make to its application in an energy production chain for dedicated operation for isolated sites. The role of stand-alone systems is to supply one or more consumers located in an isolated area of the electricity grid. The proposed system is modeled and simulated using Matlab / Simulink software to examine the dynamic characteristics of the system with the proposed control strategy. A controller is specifically designed to maintain constant dc bus voltage under wind speed and electrical load variations. The results of the modeling and simulations show that most of the isolated sites can be supplied with clean energy. Dynamic control of the dc-bus voltage has also been successfully demonstrated under varying load. A ramp dc-bus voltage reference is chosen and it is shown that the ramp slope is a deciding factor for successful current build-up. The simulation results ensure good dynamic control of the dc bus voltage with very small changes around its reference value.**

***Keywords*— Wind turbine, Dual-stator induction generator, Vector control, Stand-alone mode**

I. INTRODUCTION

The next exhaustion of fossil fuels has contributed to the development of renewable energy in general and wind energy in particular [1]. For wind energy conversion system, recent research has been focused chiefly on squirrel-cage induction generators because they are the most robust rugged and economic reasons would dictate their deployment in remote wind-farms [2].

Shunt capacitors were traditionally used to supply reactive power but back-to-back voltage source converters were necessary to ensure maximal power extraction under variable wind speed. Initial voltage in the dc bus is derived from the terminal voltage of the unexcited machine, derived from remanent magnetism of the magnetic core. Machine flux was ramped up from this small initial voltage using scalar control although no analytical justification of the ramp slope was provided [3-4]. For voltage build-up, a ramp reference of defined slope is used for the dc voltage and the selection of slope is explained analytically.

The present work is inserted in this context, which consists of control in stand-alone wind energy conversion system using vector control of Dual-Stator Induction Generator (DSIG). This last shows, in addition to the advantages of cage induction motors, other benefits, such as conventional segmentation power, high reliability [5]. The mathematical model of the turbine and the DSIG, vector control, sharing of powers between the wind system and the stand-alone network will be studied and detailed. The simulation results are presented to shown the performance of the proposed system fig.1. The above study offer various possibilities of power generation in isolated system.

II. SYSTEM CONFIGURATION AND MODELING

The basic device to be studied is that of Figure 1. This device is made up of a double stator induction generator, converter and a capacitor is connected on the power supply side of controlled converter, this makes it possible to obtain a standalone operation.

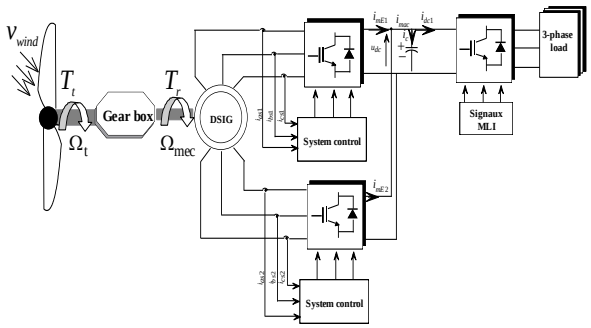

Fig 1. Scheme of the studied device

III. SYSTEM MODELLING

A. Wind turbine model

A wind turbine can only convert a certain percentage of the captured wind power. This percentage is represented by C_p which is a function of the wind speed, the turbine speed and the pitch angle of any specific wind turbine blades [6-7]. The mechanical power (P_t) extracted from the wind is mainly governed by three quantities namely: the area swept by rotor

ISSN 2356-5608

blades (*S*), the upstream wind velocity (v_{wind}) and the rotor power coefficient (C_p) by following equation:

$$P_t = \frac{1}{2} C_p(\lambda) S v_{wind}^3 \quad (1)$$

Where ρ is the air density, C_P is the turbine power coefficient that is a function of tip speed ration λ defined by Eq. (2).

$$\lambda = \frac{R\Omega_t}{v_{wind}} \quad (2)$$

The rotor efficiency curve $C_P(\lambda)$ is a nonlinear function of the tip speed ratio (TSR), λ, which is determined by the blade design, and the pitch angle [8].

From Fig.2, it is clear that there is a value of λ for which C_P is maximized, thus maximizing the power for a given wind speed. Because of the relationship between C_P and λ, for each wind velocity, there is a turbine speed that gives a maximum output power.

The turbine torque is the ration of the output power to the shaft speed Ω_t:

$$T_t = \frac{P_t}{\Omega_t} = C_P(\lambda) \frac{\rho}{2} S v_{wind}^3 \frac{1}{\Omega_t} \quad (3)$$

The torque and shaft speed of the wind turbine, referred to the generator side of the gearbox are given by following equations:

$$\Omega_t = \frac{\Omega_{me}}{G} \quad (4)$$

$$T_r = \frac{T_t}{G} \quad (5)$$

With: G: Gear box ratio

In this paper, a functional block diagram model of the turbine and power coefficient for the wind turbine model reported in [9] is used.

B. Modeling of dual-stator induction generator (DSIG)

DSIG depends on the rotational speed of the rotor. If the latter is slightly greater than that of the magnetic field of the stator, it then develops an electromagnetic force similar to that obtained with a synchronous generator. On the other hand, the machine does not generate its own excitation energy. For that, it will be necessary to bring this energy either by a battery of capacitors, or by a static converter control, which will stabilize its output voltage and frequency through capacitors connected across the stator. The model of dual-stator induction machine (DSIM) is composed of a two-phase electrical phase windings shifted by an electric angle α = 30 °, and a rotor cage squirre. [9-10].

$$\begin{cases} v_{ds1} = R_{s1} i_{ds1} + \frac{d}{dt}\varphi_{ds1} - \omega_s \varphi_{qs1} \\ v_{qs1} = R_{s1} i_{qs1} + \frac{d}{dt}\varphi_{qs1} + \omega_s \varphi_{ds1} \\ v_{ds2} = R_{s2} i_{ds2} + \frac{d}{dt}\varphi_{ds2} - \omega_s \varphi_{qs2} \\ v_{qs2} = R_{s2} i_{qs2} + \frac{d}{dt}\varphi_{qs2} + \omega_s \varphi_{ds2} \\ v_{dr} = R_r i_{dr} + \frac{d}{dt}\varphi_{dr} - (\omega_s - \omega_r)\varphi_{qr} \\ v_{qr} = R_r i_{qr} + \frac{d}{dt}\varphi_{qr} + (\omega_s - \omega_r)\varphi_{dr} \end{cases} \quad (6)$$

The expressions for stator and rotor flux linkages are

$$\begin{cases} \varphi_{ds1} = L_{s1} i_{ds1} + L_m (i_{ds1} + i_{ds2} + i_{dr}) \\ \varphi_{qs1} = L_{s1} i_{qs1} + L_m (i_{qs1} + i_{qs2} + i_{qr}) \\ \varphi_{ds2} = L_{s2} i_{ds2} + L_m (i_{ds1} + i_{ds2} + i_{dr}) \\ \varphi_{qs2} = L_{s2} i_{qs2} + L_m (i_{qs1} + i_{qs2} + i_{qr}) \\ \varphi_{dr} = L_r i_{dr} + L_m (i_{ds1} + i_{ds2} + i_{dr}) \\ \varphi_{qr} = L_r i_{qr} + L_m (i_{qs1} + i_{qs2} + i_{qr}) \end{cases} \quad (7)$$

The electrical model is completed by this mechanical equation:

$$T_{em} - T_r = J \frac{d\Omega_{mec}}{dt} + k_f \Omega_{mec} \quad (8)$$

The electromagnetic torque expression as a function of stator currents and rotor flux is as follows:

$$T_{em} = p \frac{L_m}{L_m + L_r} \left[(i_{qs1} + i_{qs2}) \varphi_{dr} - (i_{ds1} + i_{ds2}) \varphi_{qr} \right] \quad (9)$$

IV. MODELING OF DSIM FIELD-ORIENTED CONTROL OF THE DUAL-STATOR INDUCTION GENERATOR

The main objective of the vector control of induction motors is, as in DC machines, to independently control the torque and the flux [9]. In this order, we propose to study the FOC of the DSIM. The control strategy used consists to maintain the quadrate component of the flux null ($\varphi_{qr}=0$) and the direct flux equals to the reference ($\varphi_{dr}=\varphi_r^*$):
φ_r^* and the torque T_{em}^* as well as:

$$\begin{cases} \varphi_{dr} = \varphi_r^* \\ \varphi_{qr} = 0 \\ \frac{d}{dt}\varphi_r^* = 0 \end{cases} \quad (10)$$

Substituting (10) into (6) yields

ISSN 2356-5608

$$i_{dr} = 0 \tag{11}$$

$$i_{qr} = -\frac{\omega_{gl}^{*}\varphi_r^{*}}{R_r} \tag{12}$$

With: ω_{gl}*=ω_s*-ω_r (ω_{gl}*is the slip speed).

After calculation and rearrangement of the electromagnetic torque and stator voltages equations, following expressions are obtained

$$i_{dr} = \frac{\varphi_r^{*}}{L_m + L_r} - \frac{L_m}{L_m + L_r}\left(i_{ds1} + i_{ds2}\right) \tag{13}$$

$$i_{qr} = -\frac{L_m}{L_m + L_r}\left(i_{qs1} + i_{qs2}\right) \tag{14}$$

Substituting (14) into (12), obtain

$$\omega_{gl}^{*} = \frac{R_r L_m}{\left(L_m + L_r\right)}\frac{\left(i_{qs1} + i_{qs2}\right)}{\varphi_r^{*}} \tag{15}$$

The final expression of the electromagnetic torque is

$$T_{em}^{*} = p\frac{L_m}{L_m + L_r}\left(i_{qs1} + i_{qs2}\right)\varphi_r^{*} \tag{16}$$

With taking into the rotor field orientation, the stator voltage equations (6) can be rewritten as

$$\begin{cases} v_{ds1}^{*} = R_{s1}i_{ds1} + L_{s1}\dfrac{d}{dt}i_{ds1} - \omega_s^{*}\left(L_{s1}i_{qs1} + \tau_r\varphi_r^{*}\left(\omega_s^{*} - \omega_r^{*}\right)\right) \\ v_{qs1}^{*} = R_{s1}i_{qs1} + L_{s1}\dfrac{d}{dt}i_{qs1} + \omega_s^{*}\left(L_{s1}i_{ds1} + \varphi_r^{*}\right) \\ v_{ds2}^{*} = R_{s2}i_{ds2} + L_{s2}\dfrac{d}{dt}i_{ds2} - \omega_s^{*}\left(L_{s2}i_{qs2} + \tau_r\varphi_r^{*}\left(\omega_s^{*} - \omega_r^{*}\right)\right) \\ v_{qs2}^{*} = R_{s2}i_{qs2} + L_{s2}\dfrac{d}{dt}i_{qs2} + \omega_s^{*}\left(L_{s2}i_{ds2} + \varphi_r^{*}\right) \end{cases} \tag{17}$$

$$\tau_r = \frac{L_r}{R_r}$$

Where

Consequently, the electrical and mechanical equations for the system after these transformations in the space control may be written as follows:

$$\begin{cases} \dfrac{d}{dt}i_{ds1} = \dfrac{1}{L_{s1}}\left(v_{ds1}^{*} - R_{s1}i_{ds1} + \omega_s^{*}\left(L_{s1}i_{qs1} + \tau_r\varphi_r^{*}\left(\omega_s^{*} - \omega_r^{*}\right)\right)\right) \\ \dfrac{d}{dt}i_{qs1} = \dfrac{1}{L_{s1}}\left(v_{qs1}^{*} - R_{s1}i_{qs1} - \omega_s^{*}\left(L_{s1}i_{ds1} + \varphi_r^{*}\right)\right) \\ \dfrac{d}{dt}i_{ds2} = \dfrac{1}{L_{s2}}\left(v_{ds2}^{*} - R_{s2}i_{ds2} + \omega_s^{*}\left(L_{s2}i_{qs2} + \tau_r\varphi_r^{*}\left(\omega_s^{*} - \omega_r^{*}\right)\right)\right) \\ \dfrac{d}{dt}i_{qs2} = \dfrac{1}{L_{s2}}\left(v_{qs2}^{*} - R_{s2}i_{qs2} - \omega_s^{*}\left(L_{s2}i_{ds2} + \varphi_r^{*}\right)\right) \end{cases} \tag{18}$$

$$\frac{d}{dt}\varphi_r = -\frac{R_r}{\left(L_r + L_m\right)}\left(\varphi_r + L_m\left(i_{ds1} + i_{ds2}\right)\right) \tag{19}$$

$$\frac{d}{dt}\Omega_{mec} = \frac{1}{J}\left(\frac{pL_m\left(i_{qs1} + i_{qs2}\right)\varphi_r^{*}}{\left(L_r + L_m\right)} - T_g - f\,\Omega_{mec}\right) \tag{20}$$

For perfect decoupling, stator current control loops $\left(i_{ds1}, i_{qs1}, i_{ds2}, i_{qs2}\right)$ are added and at their outputs the voltage $\left(v_{ds1}, v_{qs1}, v_{ds2}, v_{qs2}\right)$ are obtained. The block control diagram is shown in Figure 2.

Dynamic equation for the dc bus voltage, shown in Figure 1, is derived as follows. Equating currents at the dc bus voltage, the following governing equation is obtained:

$$i_{dc} = C_{dc}\frac{d}{dt}v_{dc} \tag{21}$$

Block diagram of current control

The current control scheme is given in Figure 3. The references i_d* and i_q* are the outputs of the PI used in the external loop of voltage regulation v_{ld} et v_{lq}. This regulation loop allows to set the amplitude of the voltage is v_{ld}^{*} and void $i_{lq.}$

$$i_d^{*} = (PI)(v_d^{*} - v_d) \tag{22}$$

$$i_q^{*} = (PI)(v_q^{*} - v_q) \tag{23}$$

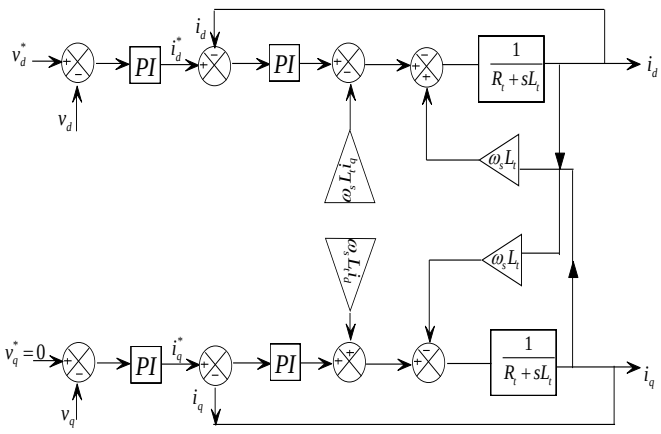

Fig 2 Current control scheme

ISSN 2356-5608

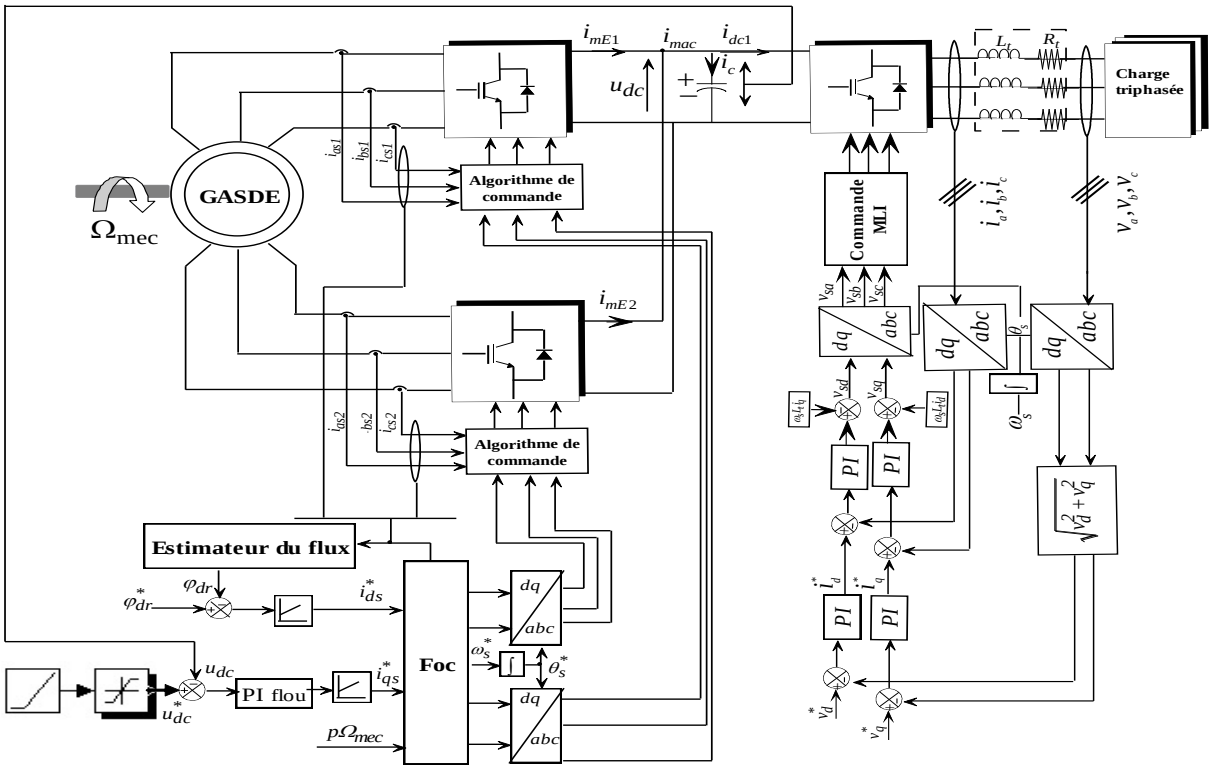

Fig 3 Control Scheme for the proposed stand-alone system

V. RESULTS AND DISCUSSION

A. *ESULTS AND DISCUSSION*

The overall system to be studied consists of a DSIG connected to a rectifier / inverter and controlled according to the control strategy presented above. In what follows, two simulation tests are performed are performed to analyze the performance of the control: The first test is dedicated to the control behavior at fixed speed control and purely resistive variable loads, the second is intended for the study of the control in the presence of an inductive load. The generator is driven at a speed of 314 rad/s with a value of voltage straightened reference u_{dc}*=622V throughout the entire duration of the simulation. The priming of the generator has taken place an empty, the presence of a remanent magnetic flux is essential or else loaded up the capacity at an initial value. In order to do this, we opted to loaded up initially the capacity an value 10 µF to 12V, to provide the reactive energy needed for priming, The q-axis current reference, generated from the voltage controller is kept at small value during starting by using the ramp voltage reference figure 4 (a and b). At the moment *t = 2s*, a balanced pure resistive three-phase load is inserted at 50% of its nominal value (*64Ω*). At the moment *t = 4s*, another load of the same characteristic as the first one is inserted at 100% of its nominal value (64Ω). The DC- link voltage follows the reference as shown in Figure 4. Figure 5 illustrates the pace of the active power that reaches almost its nominal value which is the main advantage of the studied structure.

The analysis of the figures (6-11) made it possible to see the behavior of the current, the voltage and the electromagnetic torque according to the variation of the load, where we notice that the voltage is insensitive to this variation, unlike the current and the electromagnetic torque. We notice that the torque is still in the nominal operating range.

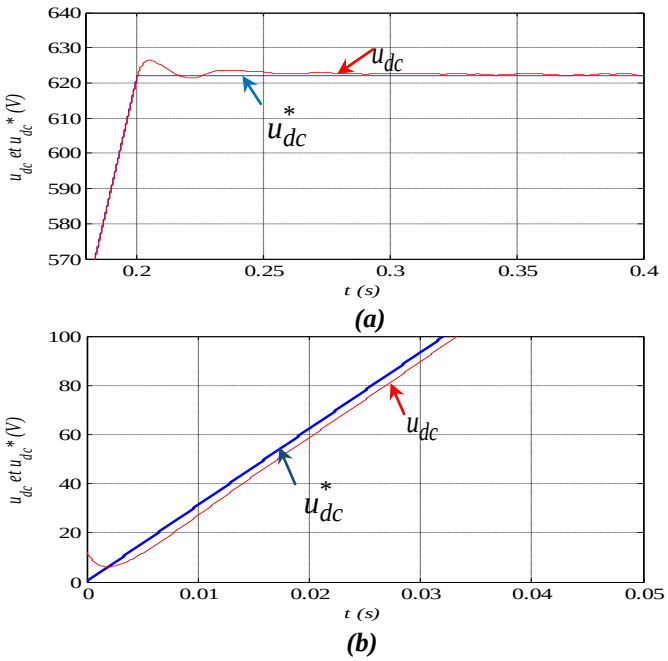

Figure 4..DC-link voltage

ISSN 2356-5608

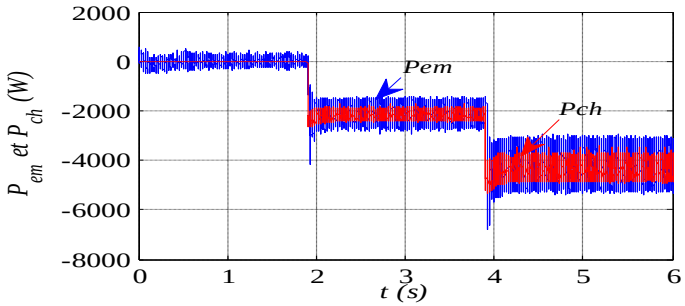

Fig5.Electromagnetic and load powers

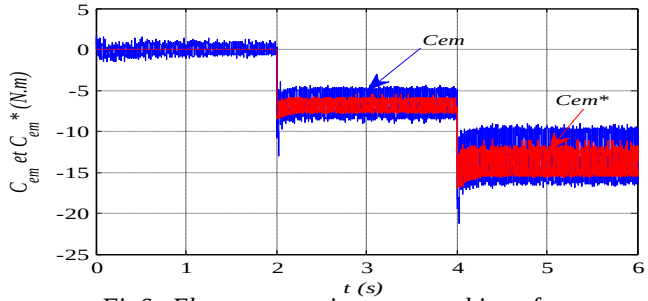

Fig6. Electromagnetic torque and its reference.

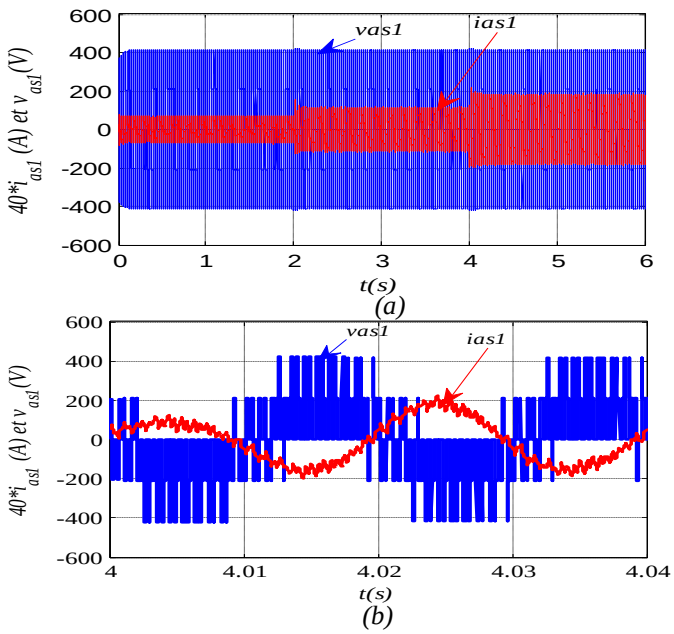

Fig7 (a) Stator voltage and current for star 1.
(b) Zoom of the stator voltage and current for star 1.

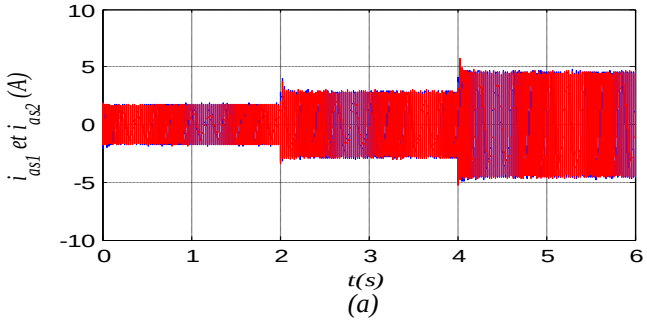

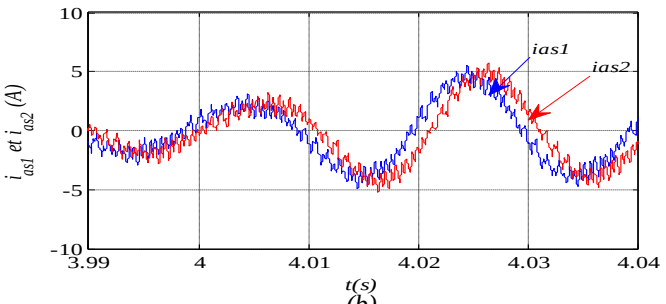

Fig 8 (a) Stator current for star 1 and 2.
(b) Zoom of the stator current for star 1and 2.

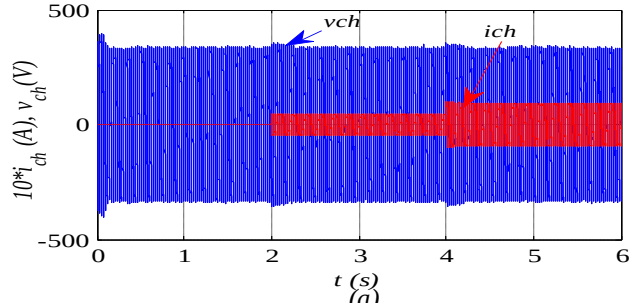

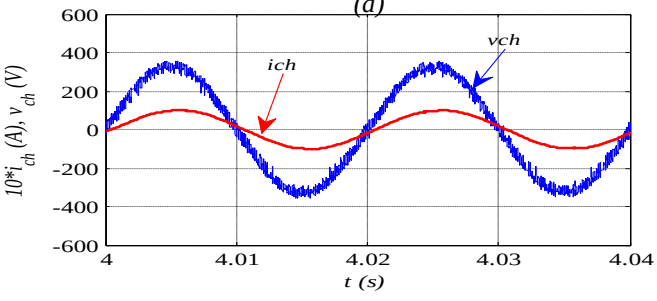

Fig 9 Voltage and current for load

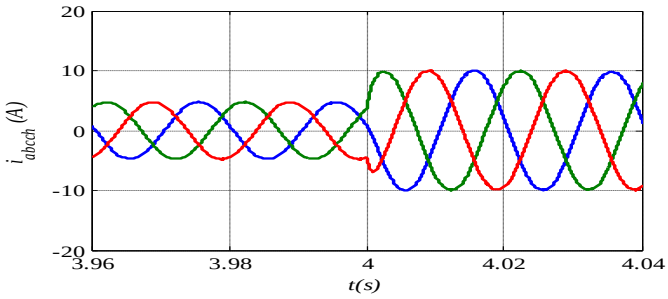

Fig10. Three-phase Load current

B. Influence of the variation of the inductive load

In this section, the performance of the GASDE is tested for an inductive load mainly consisting from the resistor (28Ω) and an inductance (50mH) per phase, while setting the drive speed at 314 rad/s. The vector control has given outstanding performance. The DC-link voltage schown in figure 11, it follows the reference. Figures [12-15] shown that active power, electromagnetic torque, voltages and stator currents are insensitive to the variation of the inductive load. Figure 16 shows the evolution of the load current and voltage, this last shown that the current in behind phase relative to voltage. In that event, we say that the stator provides active power.

ISSN 2356-5608

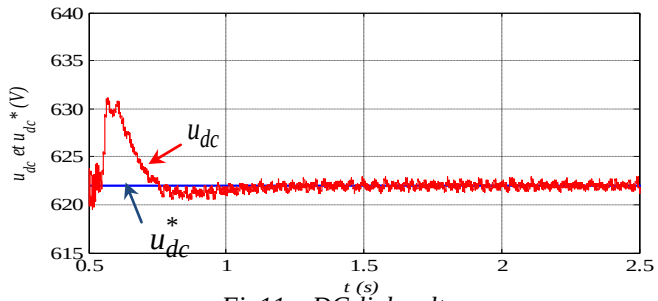

Fig11. DC-link voltage

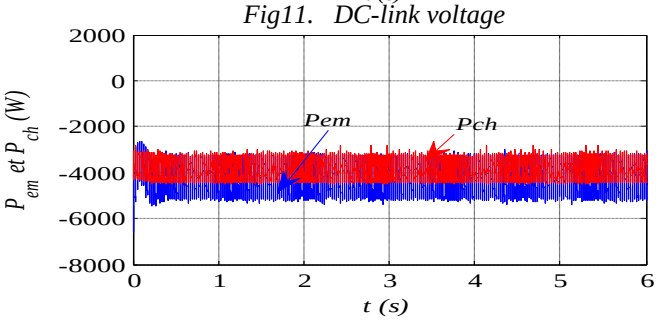

Fig12. Electromagnetic and load powers

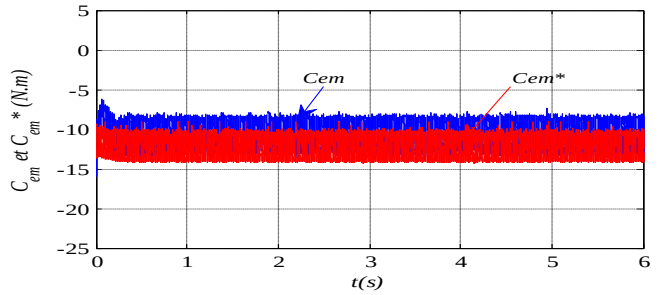

Fig13. Electromagnetic torque and its reference.

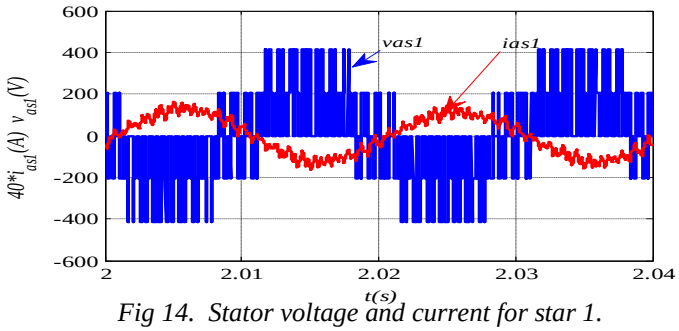

Fig 14. Stator voltage and current for star 1.

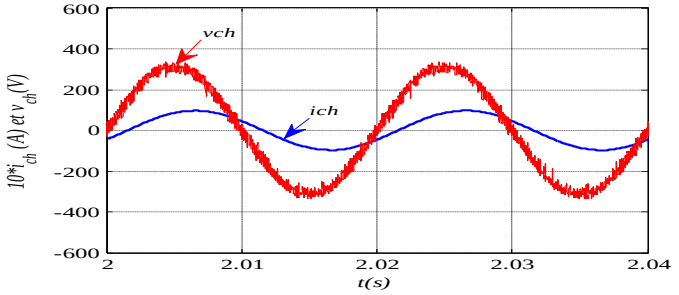

Fig15. Voltage and current for load

VI. CONCLUSION

In this paper, the subject consists of improving the performance of wind turbines based on double-star asynchronous machines operating on isolated load.

A control structure of DSIG operating in autonomous sites is presented. The description of the latter is presented, adopting a mathematical model that defines the different equations describing the operation of the machine.

The generator is connected to the converter for the control of the voltage in the presence of the variations of the load.

Dynamic control of the dc-bus voltage has also been successfully demonstrated under varying load. A ramp dc-bus voltage reference is chosen and it is shown that the ramp slope is a deciding factor for successful current build-up. The simulation results ensure good dynamic control of the dc bus voltage with very small changes around its reference value.

VII. REFERENCES

[1] Seyoum, D, Grantham ,C, Rahman, M. F. The dynamic characteristics of an isolated self-excited induction generator driven by a wind turbine. IEEE Trans on Indus Appl. 2003;39: 936–944.

[2] [Cardenas, R, Pena, R.. Sensorless vector control of induction machines for variable-speed wind energy applications IEEE Trans Energy Convers 2004; 19:196–205.

[3] Hazra, S, Sensarma, P. Vector approach for self-excitation and control of induction machine in stand-alone wind power generation IET Renew. Power Generation 2011: 5:397–405.

[4] Hazra, S, Sensarma, P.S. Self-excitation and control of an induction generator in a stand-alone wind energy conversion system IET Renew. Power Gener 2010; 4: 383–393.

[5] Hadiouche, D, Razik, H , Rezzoug, A. On the Modeling and Design of Dual-Stator Windings to Minimize Circulating Harmonic Currents for VSI fed AC Machines IEEE Trans. Ind. Appl 2004; 40.

[6] Ghedamsi K, Aouzellag D. Improvement of the performances for wind energy conversions systems. Int J Electr Power Energy Syst 2010;32(9):936–45.

[7] Aouzellag D, Ghedamsi K, Berkouk EM. Network power flux control of a wind generator. J Renewable Energy 2009;34:615–22.

[8] Poitiers F, Bouaouiche T, Machmoum M. Advanced control of a doubly-fed induction generator for wind energy conversion. Electric Power Syst Res 2009;79:1085–96.

[9] Chekkal, S, Aouzellag Lahaçani, N, Aouzellag, D , Ghedamsi K. Fuzzy logic control strategy of wind generator based on the dual-stator induction generator, International Journal of Electrical Power and Energy Systems IJEPES 2014: 59:166–175.

[10] Chekkal S, Aouzellag D, Ghedamsi K, Amimeur H. New control strategy of wind generator based on the dual-stator induction generator. In: 10th International Conference on Environment and Electrical Engineering (EEEIC), Italy; 2011. p.268–71.

[11] Singh, GK. Modeling and experimental analysis of a self-excited six-phase induction generator for stand-alone. International Journal of Research and Engineering Science direct, Renewable Energy Generation 2008 ;33:1605–21.

[12] Singh, G.K, Senthil Kumar,A, Saini, R.P. Performance evaluation of series compensated self-excited six-phase induction generator for stand-alone renewable energy generation Science direct, Energy 2010; 35 288–297.

[13] Singh, G, Senthil, A, Saini, R. Performance analysis of a simple shunt and series compensated six-phase self-excited induction generator for stand-alone renewable energy generation Science direct, Energy Conversion and Management 2011;52: 1688–1699.

ISSN 2356-5608